frontiers in Physics

REVIEW
published: 02 February 2021
doi: 10.3389/fphy.2020.631925

A Brief Review of High Efficiency III-V Solar Cells for Space Application

J. Li, A. Aierken, Y. Liu*, Y. Zhuang, X. Yang, J. H. Mo, R. K. Fan, Q. Y. Chen, S. Y. Zhang, Y. M. Huang and Q. Zhang*

School of Energy and Environment Science, Yunnan Normal University, Kunming, China

The demands for space solar cells are continuously increasing with the rapid development of space technologies and complex space missions. The space solar cells are facing more critical challenges than before: higher conversion efficiency and better radiation resistance. Being the main power supply in spacecrafts, III-V multijunction solar cells are the main focus for space application nowadays due to their high efficiency and super radiation resistance. In multijunction solar cell structure, the key to obtaining high crystal quality and increase cell efficiency is satisfying the lattice matching and bandgap matching conditions. New materials and new structures of high efficiency multijunction solar cell structures are continuously coming out with low-cost, lightweight, flexible, and high power-to-mass ratio features in recent years. In addition to the efficiency and other properties, radiation resistance is another sole criterion for space solar cells, therefore the radiation effects of solar cells and the radiation damage mechanism have both been widely studied fields for space solar cells over the last few decades. This review briefly summarized the research progress of III-V multijunction solar cells in recent years. Different types of cell structures, research results and radiation effects of these solar cell structures under different irradiation conditions are presented. Two main solar cell radiation damage evaluation models—the equivalent fluence method and displacement damage dose method—are introduced.

Keywords: III-V solar cells, multijunction, high efficiency, radaition resistance, degradation

OPEN ACCESS

Edited by:
Feng Chi,
University of Electronic Science and Technology of China, China

Reviewed by:
Changsi Peng,
Soochow University, China
Xingji Li,
Harbin Institute of Technology, China

****Correspondence:***
A. Aierken
erkin@ynnu.edu.cn
Y. Liu
542110131@qq.com

Specialty section:
This article was submitted to Optics and Photonics, a section of the journal Frontiers in Physics

Received: *21 November 2020*
Accepted: *21 December 2020*
Published: *02 February 2021*

Citation:
Li J, Aierken A, Liu Y, Zhuang Y, Yang X, Mo J H, Fan RK, Chen QY, Zhang SY, Huang YM and Zhang Q (2021) A Brief Review of High Efficiency III-V Solar Cells for Space Application. Front. Phys. 8:631925. doi: 10.3389/fphy.2020.631925

INTRODUCTION

Space solar cells, being the most important energy supply unit, have been employed in spacecrafts and satellites for over sixty years since the first satellite was launched in 1958 [1]. It has been developed from the initial single junction low efficiency silicon solar cells [2] to the now high efficiency multi-junction III-V compound multi-junction solar cells [3]. The main objectives of space solar cell development are directed toward to improving the conversion efficiency and reducing the mass power ratio and increase the radiation hardness [4–7]. At present, the highest conversion efficiency of solar cells is 47.1% achieved by six-junction inverted metamorphic (6 J IMM) solar cells under 143 suns [8]. The high-efficiency III-V triple-junction cells are also becoming the mainstream of space solar cells. The best research-grade multi-junction space solar cell efficiency so far is 35.8% for five-junction direct bonded solar cell and 33.7% for the monolithically grown 6 J IMM multi-junction solar cell [9, 10]. Despite the high fabrication cost, they offer excellent performance and reliable stability for space missions [11–13]. GaInP/GaAs/Ge (1.82/1.42/0.67 eV) lattice-matched triple-junction cells are well established with efficiencies of over 30% and fulfilled many space applications in the past two decades. However, the current mismatch between its subcells makes it difficult to improve the conversion efficiency further [14]. New structures of current matched or

lattice mismatched solar cell structures and different fabrication methods are proposed to overcome this problem, such as the metamorphic (MM) growth method [15], mechanical stack [16], wafer bonding technology [17], etc.

While improving the efficiency of space solar cells, the radiation resistance should also be considered. In-orbit solar cells suffer from irradiation damages due to high energy protons and electrons in the earth's radiation belt and cosmic rays [18, 19], and consequently, the photoelectric performance of solar cells will be degraded. The main reason of the degradation of solar cell performance is due to the radiation-induced displacement damage in the solar cell lattice, resulting in a decrease in the lifetime of the photo-generated carriers [20–22]. Therefore, the degradation mechanism and performance of solar cells under an irradiation environment must be explored, and it is necessary to apply radiation hardening methods before the space mission starts. The degradation of electrical performance in solar cells directly affects the life-time of space missions. The researchers aimed at improving the radiation resistance of solar cells by adding a certain thickness of protective cover to the solar cell to shield the damage of certain particles [23], using back-surface (BSF) [24] or distributed Bragg reflector (DBR) [25], and thinning the base layer thickness of the current-limiting subcell [26], or using the p-i-n structure and different doping methods for multi-junction solar cells [27]. The experimental observations show that annealing of the multi-junction solar cell can restore certain electrical properties after being radiated by high-energy particles [28].

In recent years, various new types of multi-junction solar cells with different combinations of materials have been developed by different research groups, and the expectations for future development are different. Solar cell conversion efficiencies are rapidly being updated, and scientists are still struggling to come up with solar cells which have high conversion efficiency and possess good radiation resistance. Although there are several reviews available which cover the manufacturing, efficiency, and application prospects of photovoltaic modules [29, 30], the new types of high efficiency space solar cells based on III-V compound materials have not been summarized yet. This review attempts to give a brief review on different types of space solar cells and emphasize the high energy particle irradiation effects of solar cells and recent results on the most promising types of solar cells, including dilute nitride, metamorphic, mechanical stack, and wafer bonding multi-junction solar cells.

DIFFERENT TYPES OF HIGH-EFFICIENCY SOLAR CELLS

With the improvement of the manufacturing process and deposition technology of materials, the solar cells industry has developed tremendously. Solar cell materials are developed from a single material (single crystal Si, single-junction GaAs, CdTe, CuInGaSe, and amorphous Si:H) to compound materials, such as III-V multi-junction solar cells, perovskite cells, dye-sensitized cells, organic cells, inorganic cells, and quantum dot cells [31–33]. The structure of solar cells also forms homogeneous junction cell to heterogeneous junction solar cell, Schottky junction solar cell, compound junction solar cell, and liquid junction solar cell. In the purpose of its usage, it has also been developed from flat cells to concentrator cells and flexible cells [34, 35].

The silicon solar cells were used as the first choice in the spacecraft since the first solar-powered satellite was launched in 1958. The Soviet Space station, MIR, was launched in 1986, was equipped with 10 kW GaAs solar cells, and the power per unit area reached 180 W/m^2 [36]. Then, the fabrication technique of GaAs-based cells experienced changes from Liquid Phase Epitaxy (LPE) to metal organic vapor phase epitaxy (MOVPE), from homogeneous epitaxy to heterogeneous epitaxy, from single junction to multi-junction structure [37–39]. Notably, their efficiency was continuously improved from the initial 16–25%, and over 100 kW industrial-scale power output per year has been reached [40]. Higher efficiency reduces the size and weight of the array, increases the payload of the spacecraft and results in lower costs for the entire satellite power system. Therefore, GaAs-based solar cells are widely used in space systems and continue to be used today [41–43]. Comparing with silicon solar cells, GaAs solar cells have the following advantages [42]:

(1) Higher photoelectric conversion efficiency.
(2) Direct-gap semiconductor materials.
(3) The band-gap tailoring by controlling the composition and doping of material.
(4) Superior radiation resistance.

However, the processes involved in GaAs solar cell fabrication are complicated, and its cost is much higher than that of silicon solar cells owing to the expensive equipment and material preparation. Therefore, GaAs solar cells cannot be widely utilized in the civil market. Nevertheless, GaAs solar cells have gradually replaced silicon solar cells in the aerospace field, where higher cell efficiency and better radiation resistance are needed.

The loss in the efficiency of solar cells can be divided into two parts: the unabsorbed loss and excessive energy loss. When the photon interacts with the semiconductor materials, where the photon energy is smaller than the bandgap width, the valence band electrons are not excited, and they do not generate an electron-hole pair to form an electrical current. However, when the photon energy is greater than the gap width, the excess energy is lost in the form of phonons or heat [44]. Fortunately, multi-junction solar cells successfully solved this problem. Semiconductor materials with different band-gaps are composed from top to bottom from large to small band-gaps, and the higher energy photons are absorbed by the top large band-gap material. The lower energy photons go through the upper large band-gap material and reach the appropriate band-gap width to generate power. Therefore, for multi-junction solar cells, finding a current matching and lattice matching cell material is the critical and general focus [14, 45]. The following sections present a brief introduction of different types of multijunction solar cells in terms of their performance.

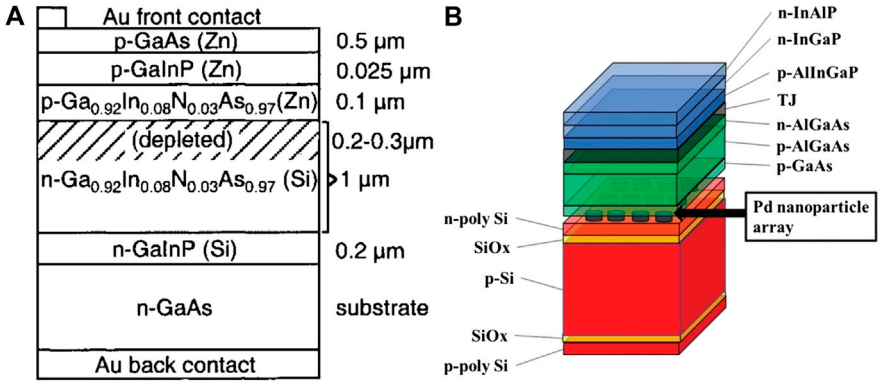

FIGURE 1 | (A) The structure of GaInNAs device grown by MOVPE with dimethylhydrazine as the nitrogen source [50]; **(B)** The structure of InGaP/AlGaAs//Si triple-junction solar cell [67].

TABLE 1 | The parameters of GaInAsN solar cell after 1 MeV electron irradiation [51].

Fluence	V_{oc} (%)	FF (%)	J_{sc} (%)	Power (%)
5×10^{14}	97.7 ± 1	98.6 ± 1	97 ± 3	93 ± 3
1×10^{15}	96.2 ± 1	97.8 ± 1	95 ± 4	89 ± 4

Lattice Matched GaInNAs Multi-Junction Solar Cell

In 1996, Kondow et al. demonstrated the epitaxial growth of 1.0 eV band gap GaInNAs material with lattice matching to GaAs substrate, and applied it to fabricating infrared laser [46]. Since then diluted nitride GaInNAs materials have been widely used in heterojunction bipolar transistors (HBTs) [47] and lasers [48], where GaInNAs HBTs base layer can reduce the open voltage and run under low working voltage. These features of diluted nitride GaInNAs materials are also useful in wireless communications and power amplifier applications. GaInAsN is a direct band-gap semiconductor material, which can change its band-gap by adjusting the component content of nitrogen and indium while keeping its lattice constant matching to conventional substrate materials such as GaAs and Ge. These advantages bring great potential for using 1.0 eV subcell in a high efficiency multijunction solar cell [49].

The $Ga_{1-x}In_xN_yAs_{1-y}$ is used as a sub-cell material for GaInP/GaAs/GaInNAs/Ge four-junction solar cell by NREL [50]. When y = 0.3x, the lattice constant of $Ga_{1-x}In_xN_yAs_{1-y}$ matches GaAs and Ge, which is an ideal material to construct a GaInP/GaAs/GaInNAs/Ge (1.88/1.42/1.05/0.67 eV) four-junction solar cell with band-gap matching. **Figure 1A** shows the representative GaInNAs devices structure grown by MOVPE. The device is grown with dimethylhydrazine (DMHy) as the nitrogen source. At the same time, the experimental results showed that the remaining factor of GaInAsN cell efficiency is 0.93 and 0.89 after 5×10^{14} and 1×10^{15} e/cm^2 electron fluence of 1 MeV electrons irradiation, respectively [51]. The specific degradation of the device parameters is summarized in **Table 1**. The results showed that this type of cell structure possesses superior radiation resistance comparing to the traditional lattice matched multi-junction solar cell.

However, difficulties in epitaxial growth of diluted nitride materials have prevented its further development. It is also found that the diffusion length of minority carriers is short, the internal quantum efficiency is low for the GaInNAs subcell, and these poor minority carrier transmission characteristics resulted in lower current and voltage. Since the current of a multi-junction solar cell is determined by the smallest sub-cell, the low current in GaInNAs subcell has a significant impact on the overall cell performance [51]. The quality of GaInNAs solar cells was improved by fabrication of p-i-n structure cells [52], annealing [53], doping Sb in GaInNAs material [54], and changing substrate epitaxial orientation [55]. Miyashita et al. demonstrated a solar cell with p-i-n (*p*-GaAs/i-GaInAsN (Sb)/n-GaAs) structure, and tested the cell under the AM1.5 spectrum. The short-circuit current density (J_{sc}) reached 21.5 mA/cm^2, the open-circuit voltage (V_{oc}) reached 0.42 V, and the filling factor (*FF*) reached 0.71 [56]. They further optimized the content of Sb and found that the content of Sb was less than 1%, which is more beneficial to improve GaInAsN crystal quality and device performance [57]. Han et al. found that GaAsN material grown by (311) B substrate epitaxy could not only improve the incorporation efficiency of nitrogen, but also effectively enhance the carrier lifetime of the material [58]. Although the theoretical conversion efficiency of GaInNAs multijunction solar cell could reach 41%, the actual growth problem still needs to be overcome, which needs to be focused on as a development goal in the future.

Mechanically Stacked Solar Cell

According to the theoretical calculation, the optimum bandgap energy for top and bottom subcell for a tandem multijunction solar cell is 1.65–1.8 eV and 1.0–1.5 eV, respectively, and the conversion efficiency of this structure reaches 32.5% under 1-sun AM0 spectrum [59]. Typically, the III-V compound material based multijunction solar cells are fabricated by MOVPE or molecular beam epitaxy (MBE) techniques, where the lattice matching and energy matching between subcells is a critical

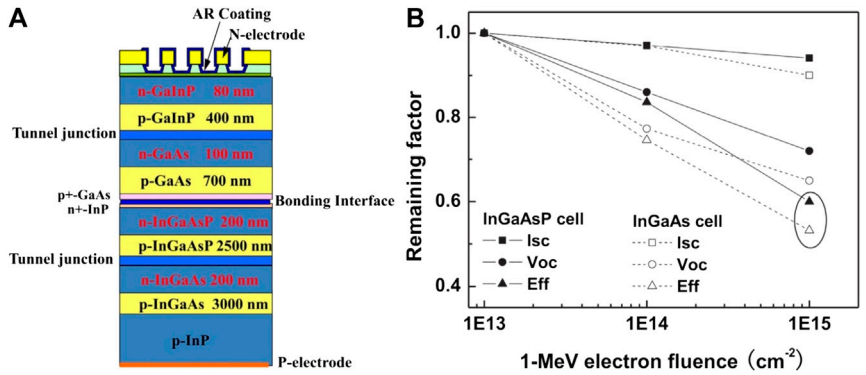

FIGURE 2 | (A) Schematic structure of wafer-bonded GaInP/GaAs//InGaAsP/InGaAs four junction solar cell; **(B)** the remaining factors of InGaAs and InGaAsP single-junction solar cells as a function of 1 MeV electron irradiation fluence **(B)** [71].

problem. The presence of mechanical stacks makes this feasible and allows to use of lattice- and current-mismatched combinations of semiconductor materials. By using the mechanical stacking method, III-V compound materials can be stacked together regardless of their bandgap energy and lattice constants. This technique can reduce the production cost significantly, and the substrate removal process greatly reduces the weight of solar cells, which is useful if used in space solar cell applications [60–62].

Still, the utilization of multiple substrates requires the removal of substrates, thereby, it makes the solar cell fabrication process complicated and affects the interface quality [63]. At the same time, a complicated design requirement becomes an obstacle for large-scale applications of mechanical stacked solar cells in space [64]. Since each subcell in a multi-junction solar cell consists of a p-n junction, if individual subcells directly stacked together in series, it will form a reverse p-n junction between subcells which block the current flow. Therefore, interconnecting individually processed solar cells keeping both electrical and optical properties still is a technical challenge need to consider with high conductivity and low transmission loss [65]. This problem can be solved by adding a tunnel junction between the subcells [66]. The 30% conversion efficiency of III-V//Si multi-junction solar cells using smart stack technology have been reported [67]. A schematic diagram of InGaP/AlGaAs//Si triple-junction solar cell is shown in **Figure 1B**. A "smart stack," "areal current matching," and "solar concentration" two-terminal GaAs/Si tandem solar cell, having potential to achieve an efficiency of approximately 30%, are proposed and the indoor experiment proves its feasibility, although the experiment result is lower than the simulation [64]. These types of mechanical stacking processes are quite flexible and allow different cells to be combined, and consequently reduces the fabrication cost and increases the cell efficiency.

Wafer Bonded Multijunction Solar Cell

In multi-junction solar cells, the lattice dislocations induced by the lattice mismatch during the epitaxial growth reduce the material quality and deteriorates the device performance. The wafer bonding technique, which refers to the physical integration of the two different materials, overcomes this issue very well and allows the formation of a monolithic multijunction solar cell structure without both electrical and optical losses, regardless of the different lattice constant of subcells [68]. As early as 1986, Lasky et al. demonstrated surface treated silicon wafer bonding at room temperature and obtained very good bonding strength through high-temperature annealing [69]. The freedom of material selection in the process of semiconductor device design is greatly improved because the bonding technology can realize the lamination structure of materials with different thermal expansion coefficient and lattice constant, and can limit the dislocation and defect to the area near the bonding interface. **Figure 2A** shows the structure of GaInP/GaAs//InGaAsP/InGaAs wafer-bonded four junction solar consists of GaInP/GaAs and InGaAsP/InGaAs dual junction cells, whereas **Figure 2B** shows the degradation of InGaAsP and InGaAs subcell electrical properties under 1 MeV electron irradiation. The result shows that the bonding interface has no effects on overall cell performance and radiation resistance, the main degradation happened in the third and fourth subcell, and InGaAsP subcell has a superior radiation resistance than InGaAs cell owing to In-P bonds [70].

At present, the wafer bonding technology has been studied extensively and widely used in the structural design and integration field of microelectronics and optoelectronics. A variety of bonding methods have been developed, however, they can be mainly divided into two categories: direct bonding and intermediate-layer bonding [71]. The direct wafer bonding process includes cleaning and activating two polished wafers and sticking them together at room temperature. Heterogeneous integration of multi-junction solar cells has to meet three stringent conditions: good mechanical strength at the bonding interface, high optical transmittance, and low resistivity. It does not work without each condition being met. Intermediate-layer bonding technology introduces a layer with good ductility and adhesion to alleviate stress and improve the bonding interface [72]. GaInP/GaAs//GaInAsP/GaInAs four-junction wafer-bonded concentrator solar cells with an efficiency of 46% at 508 suns have been reported [73]. It demonstrates that the wafer bonding is a feasible method to combine lattice mismatched

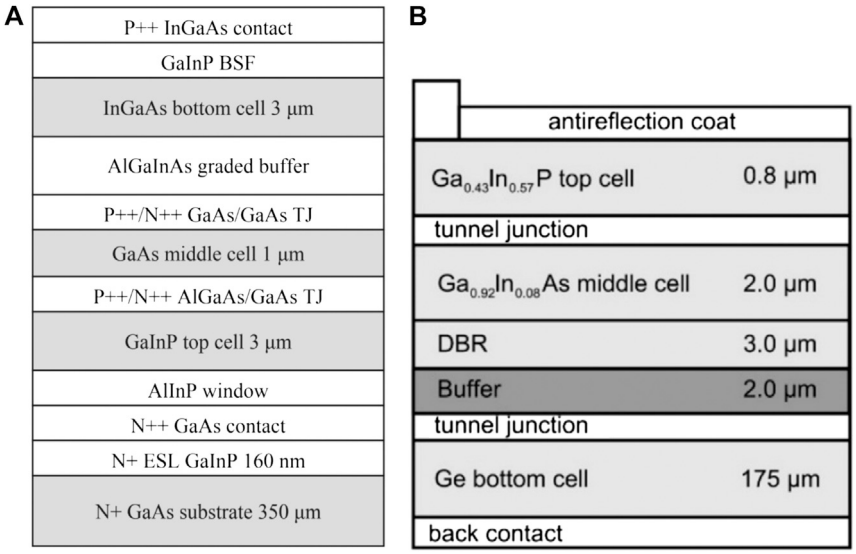

FIGURE 3 | Schematic structure of **(A)** GaInP/GaAs/InGaAs IMM solar cell, and **(B)** GaInP/InGaAs/Ge UMM solar cell [78].

different III-V compound materials and realize high efficiency multijunction solar cell structure. The main challenge of wafer bonding technology is the preparation of the bonding surface which should have a low surface roughness to ensure high electrical conductivity.

Inverted Metamorphic and Upright Metamorphic Solar Cells

Another approach of solving current matching issue in multijunction solar cell is the metamorphic growth method, which involves applying a compositionally graded buffer (CGB) layer between the lattice mismatched subcells [74]. The main purpose of using a CGB layer is to distribute the strain relaxation layers into a lattice constants gradually changed thick buffer layer instead of growing a highly lattice mismatched layer onto its under layer [75]. According to the growth method, the metamorphic growth technique can be divided into two types: IMM [76] and upright metamorphic (UMM) [77]. In the IMM method, for example GaInP/GaAs/InGaAs triple junction solar cell, a CGB layer is inserted between the GaAs and InGaAs subcells and the growth direction of solar cell epilayers is in the inverse direction, in order to delay the strain relaxation in CBG layer at the later stages of growth process. However, the IMM method requires an additional step of substrate lift-off before solar cell device fabrication processes. On the other hand, in the UMM method, the growth direction is from bottom subcell to top subcell, so it requires an even higher quality CBG layer to control the strain relaxation. **Figures 3A,B** show the general structure of IMM and UMM cells, respectively.

Comparing to traditional lattice matched (LM) solar cells, metamorphic multijunction solar cells are aiming to achieve current matching between its subcells and expected to have higher conversion efficiency. Experimentally, NREL has shown that IMM solar cells have a conversion efficiency of 40.8% for triple-junction solar cells at high concentration [15] and 47.1% efficiency for 6 J solar cells at 143 suns concentration [8]. Furthermore, IMM cell can reduce the cell weight by removing the substrate and increase the mass power ratio. IMM cells also can be utilized to develop flexible solar cells for any non-flat surfaces. These high efficiency, flexible, and lightweight properties of IMM multi-junction solar cells make them the most promising for space applications [[14, 78, 79]]. For UMM multijunction solar cell, the conversion efficiency exceeded 31% under one Sun AM0 spectrum compared to traditional lattice matched solar cell conversion efficiency is limited to 30% [80]. The critical point of increasing UMM solar cells is improving the quality of CGB layer to suppress lattice dislocation and threading dislocations induced by strain relaxation. However, the fabrication process of UMM solar cells is similar to the matured fabrication technology of LM cells, therefore, this advantage makes the UMM multi-junction solar cell utilization possible for potential applications [77].

The reported experimental efficiency, theoretical limits, and their advantages of all above mentioned solar cells in *Lattice Matched GaInNAs Multi-Junction Solar Cells, Mechanically Stacked Solar Cells, and Wafer Bonded Multijunction Solar Cells* are presented in **Table 2**. According to the Shockley-Queisser balance model, the theoretical efficiency limit of single-junction, triple-junction, and four-junction solar cells are 33.5%, 56% and 62%, respectively [85]. Along with the rapid development of new materials and high quality fabrication technologies, all these solar cells could achieve higher efficiency and better performance. Furthermore, UMM and IMM solar cell efficiencies tend to surpass LM cells even more as their manufacturing technology continues to be innovated and developed, and they are expected to become the next generation space solar cells.

TABLE 2 | Comparison of the conversion efficiency of various types of solar cells have been reported.

Classification	Experimental efficiency (%)	Theoretical limit efficiency (%)	Technical advantages
Si	26.7 ref. 81	33.5	Mature technology, rich output
GaAs	29.1 ref. 82	33.5	High temperature, better resistance, mature technology
GaInP/GaAs/GaInNAs/Ge	27.4 ref. 50	62.0	Band-gap matching, superior radiation resistance
InGaN	3.4 ref. 83	33.5	Adjustable band-gap
GaInP/GaAs/Ge (LM)	30 ref. 80	56.0	Lattice matching, mature technology
GaInP/InGaAs/Ge (UMM)	31.7 ref. 84	56.0	Band-gap matching, fabrication process is similar to LM solar cell
InGaP/GaAs/InGaAs (IMM)	33.7 ref. 9	56.0	Band-gap matching, lightweight

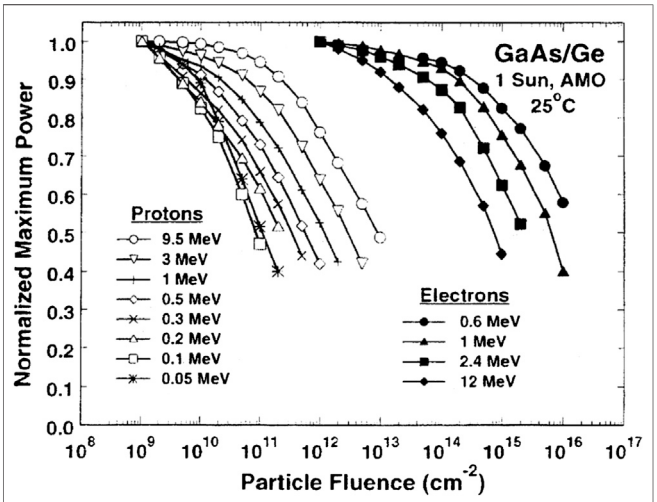

FIGURE 4 | Normalized P_{max} degradation of GaAs/Ge solar cells irradiated by electrons and protons of different energy and with different particle fluence [88].

STUDIES ON RADIATION EFFECTS OF SOLAR CELLS

The solar cell arrays in a spacecraft are exposed to a harsh space environment during its mission. Therefore, radiation resistance is also a critical index to evaluate the quality of space solar cells. The main reason for the performance deterioration of space solar cells is the irradiation of high-energy particles, that include electrons (energy up to 10 MeV) and protons (energy up to several hundred MeV) from the earth's radiation belt, as well as solar cosmic rays (energy up to GeV) [86]. When these high-energy particles collided with the cell materials, the transmitted energies cause the lattice atoms to shift their original positions and form displacement damages, and, consequently, the diffusion length of minority carriers decreases and the performance of solar cells is degraded [87]. Therefore, only solar cells with high conversion efficiency and good radiation resistance could be employed as space solar cells.

Radiation Effects of Double-Junction GaAs/Ge Solar Cell

Messenger et al. investigated the electron and proton irradiation effects of double-junction GaAs/Ge solar cell with different energies [88]. The cell performance is degraded with an increase of the particle fluence under both electron and proton irradiation, as shown in **Figure 4**. Additionally, electron irradiation with greater incident energy resulted in more severe deterioration of cell performance for the same irradiation fluence. For proton irradiation, on the other hand, low energy protons produced a bigger reduction in cell performance when the proton energy is in the range of 0.2–9.5 MeV. Proton irradiation experiments on GaInP/GaAs/Ge, GaAs/Ge solar cells with proton energy of less than 200 KeV are reported and it was found that the low energy particle irradiation caused defects in different subcells and different regions in the tandem multi-junction solar cell [23, 89].

The radiation-induced defects in the base and the emitter layers form non-radiative recombination centers and capture photo-generated electron-hole pairs before they are collected by the junction region, and eventually reduce the short circuit current. On the other hand, the radiation-induced damages in the junction region mainly cause the degradation of open circuit voltage by introducing deep energy levels into the band gap and accelerating the recombination of valence band holes and conduction band electrons [89].

The effects of 40, 100, 170 keV energy proton irradiation on GaAs/Ge cells with different fluences were discussed, the degradation of spectral response results indicated that the largest damages are caused by 170 keV protons, and the lowest by 40 keV protons, in the long wavelength range (720–900 nm). The degradation effect on the normalized maximum power (P_{max}) is the largest for the 170 keV protons and lowest for 100 keV protons because irradiation with 170 keV protons produces the most severe damage in the junction region of the cells. The short circuit current decreases with increasing proton energy under the energies of 40–170 keV proton irradiation and the degradation extent of V_{oc} is the largest for 170 keV proton because they produce defects with deep energy levels in the space charge region, accelerating the recombination of electrons and holes, which is also the reason for the significant decline in P_{max} for solar cell [23].

Radiation Effects of Lattice Matched GaInP/GaAs/Ge Triple-Junction Solar Cell

Sharps et al. investigated the electron and proton radiation effects of GaInP/GaAs/Ge solar cells with different energies [91]. Same as that of GaAs/Ge double-junction solar cell, the P_{max} of solar

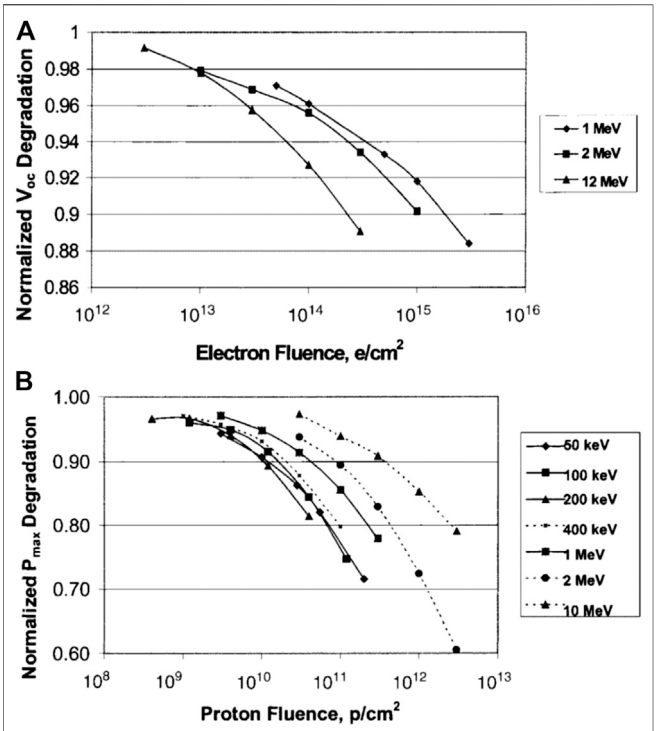

FIGURE 5 | The normalized P_{max} degradation of lattice-matched GaInP/GaAs/Ge solar cells under different **(A)** electrons and **(B)** protons irradiation with different particle fluence [91].

cells declined with the increase of the particle fluence for the same energy. For 1–12 MeV electron irradiation, the degradation of cell performance is severer for higher energy electrons for same irradiation fluence, as shown in **Figure 5A**. The degradation of P_{max} is 9 and 13% for 1 MeV electrons at fluences of 5×10^{14} and 1×10^{15} e/cm^2. However, for proton irradiation, the degradation of cell performance is bigger for lower energy protons in the energy range of 50–200 keV, as shown in **Figure 5B**. The main reason for this is that less relative damage occurs for energies below 200 keV, and lower energies would have more of an effect on the emitter as compared with the base region. At the same time, GaInP top cell and GaAs middle cell current matching point was studied in more detail by quantum efficiency measurements. It was found that the crossover from GaInP current-limited subcell to GaAs current-limited subcell occurs at 2×10^{15} e/cm^2 for the 1 MeV electrons [90]. This result indicated that advanced triple junction solar cells with current matching at end of life (EOL) can be achieved by reducing the amount of beginning of life (BOL) current mismatch, which is helpful for designing high efficiency radiation hardened space solar cells.

Wang et al. investigated the electron irradiation effects of GaInP/GaAs/Ge solar cell with 1.0–11.5 MeV energy electron beams [91]. The degradation of normalized P_{max} of GaInP/GaAs/Ge solar cell under different fluence of electron irradiation is shown in **Figure 6A**, whereas the degradation of external quantum efficiency (EQE) changes irradiated with 1.8 MeV electron beam with different fluences are shown in **Figure 6B**.

The degradation effects of electron irradiation of the P_{max} and the EQE of LM solar cells increase with the increase of irradiation fluences and electron energy, as observed in GaAs/Ge double-junction cell. **Figure 6C** exhibits that the EQE of GaAs middle cell degrades more than GaInP top cell under same irradiation fluence which is indicating the radiation resistance of GaInP/GaAs/Ge triple-junction cells is dominated by the GaAs middle cell.

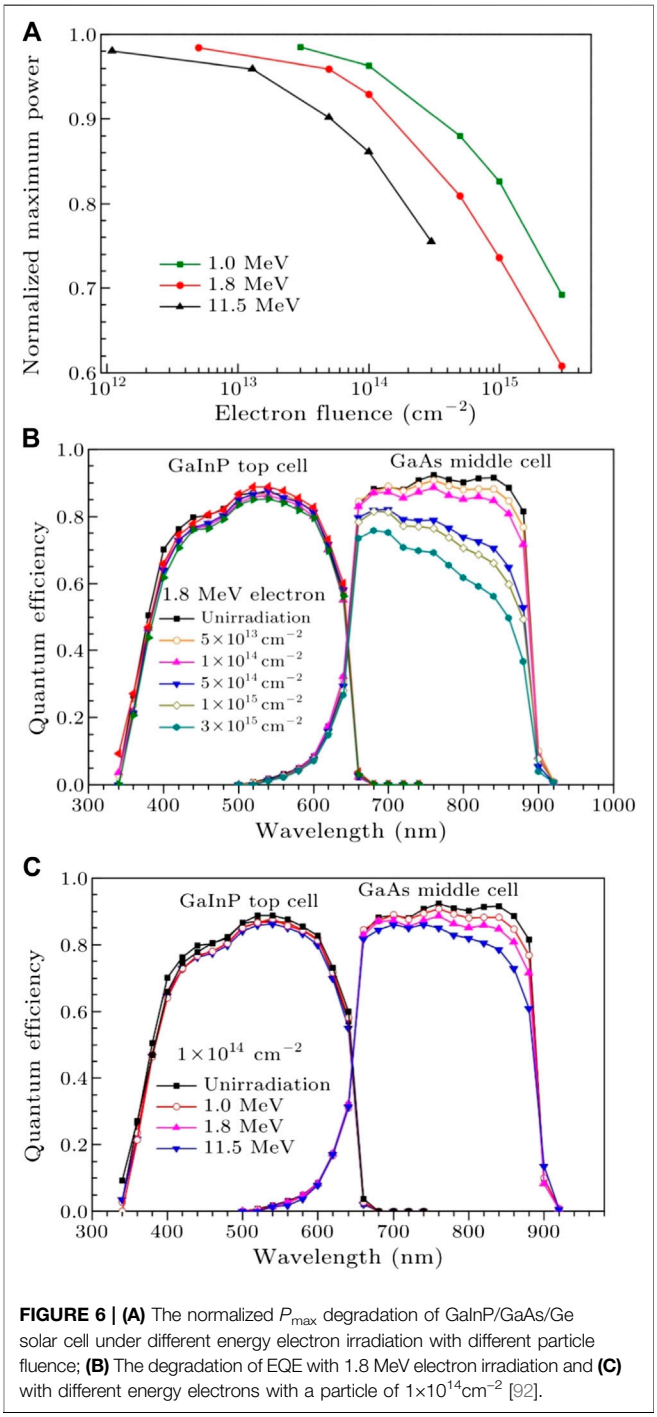

FIGURE 6 | (A) The normalized P_{max} degradation of GaInP/GaAs/Ge solar cell under different energy electron irradiation with different particle fluence; **(B)** The degradation of EQE with 1.8 MeV electron irradiation and **(C)** with different energy electrons with a particle of 1×10^{14}cm^{-2} [92].

TABLE 3 | Changes of electrical parameters of IMM GaInP/GaAs/InGaAs triple-junction solar cell under 1 MeV electron irradiation [92].

Cell type	Fluence (e/cm^2)	Voc (mV)	Jsc (mA/cm^2)	FF	Eff (%)	Remaining factor of eff (%)
GaInP/GaAs/InGaAs (higher efficiency at BOL)	0	3055.2	68.2	0.842	31.2	-
	1E15	2728.3	65.7	0.823	26.2	84.1
	3E15	2651.9	64.3	0.772	23.4	75.1
GaInP/GaAs/InGaAs (higher efficiency at EOL)	0	3058.3	67.3	0.838	30.6	-
	1E15	2709.6	66.4	0.831	26.5	86.7
	3E15	2602.8	66.3	0.794	24.3	79.5

Radiation Effects of Metamorphic GaInP/GaAs/InGaAs Triple-Junction Solar Cell

By taking advantages of bandgap tailoring in III-V compound materials and using a CGB layer, IMM multijunction solar cells can be adjusted to its output parameters suitable for BOL or EOL requirements. Takamoto et al. studied the radiation effects of these two types of IMM GaInP/GaAs/InGaAs space solar cells under 1 MeV electron irradiation, where the electrical parameters of both types solar cells declined with the increase of electron irradiation fluence [92]. In this study, the electrical parameters V_{oc}, I_{sc} (short-circuit current) and η decayed o 89.3%, 96.3%, 84.1% and 88.6%, 98.6%, and 79.5% of its original values for one group of cells have higher efficiency at BOL and another group of cells have higher efficiency at EOL, respectively, when the electron irradiation fluence reaches 1×10^{15} cm^{-2}. These details of degradation of electrical parameters of these two types of cells are summarized in **Table 3**.

Imaizumi et al. studied the radiation response of $In_{0.5}Ga_{0.5}P$, GaAs, $In_{0.2}Ga_{0.8}As$, and $In_{0.3}Ga_{0.7}As$ single-junction solar cells, whose materials are also used as component subcells of inverted metamorphic triple-junction solar cells, and results show that the photo-generation current in the InGaAs bottom subcell of InGaP/GaAs/InGaAs IMM3J cells was severely damaged under the electron and proton radiation, which can be attributed to the stronger decrease of minority-carrier diffusion length in InGaAs compared with that in InGaP and GaAs subcells after irradiation [93]. By comparing the irradiation resistance of two InGaAs cells ($In_{0.2}Ga_{0.8}As$ and $In_{0.3}Ga_{0.7}As$ cells), GaAs and InGaP cells, it was found that radiation resistance of these two InGaAs cells is approximately equivalent to InGaP and GaAs cells from the initial material qualities. However, the InGaAs cells show lower radiation resistance especially for the I_{sc} comparing to InGaP and GaAs cells due to the bigger decrease of minority-carrier diffusion length in InGaAs materials. And the InGaP and two InGaAs cells exhibited equivalent radiation resistance of V_{oc}, but with different degradation mechanisms.

Zhang et al. investigated the 1 MeV electron radiation effects of IMM GaInP/GaAs/InGaAs solar cells by electrical properties, spectral response, and photoluminescence (PL) signal amplitude analysis [94]. The results show that the electrical parameters of IMM solar cell decrease continuously with an increase in the electron fluence same as traditional LM GaInP/GaAs/Ge solar cells. As shown in **Figure 7**, P_{max} illustrates the maximum degradation compared to V_{oc} and I_{sc}, and, V_{oc} is degraded more compared to I_{sc}. This phenomenon is explained as V_{oc} is the sum of three series sub-cell voltages, where the I_{sc} is the smallest current produced in three series sub-cells. The $In_{0.3}Ga_{0.7}As$ bottom subcell exhibited most severe damage in the irradiated IMM triple junction cells due to the drastic degradation of the effective minority carrier lifetime (τ_{eff}) of $In_{0.3}Ga_{0.7}As$ subcell than that of GaAs subcell. Therefore, the radiation hardness of IMM GaInP/GaAs/InGaAs solar cell is mainly determined by the InGaAs subcell.

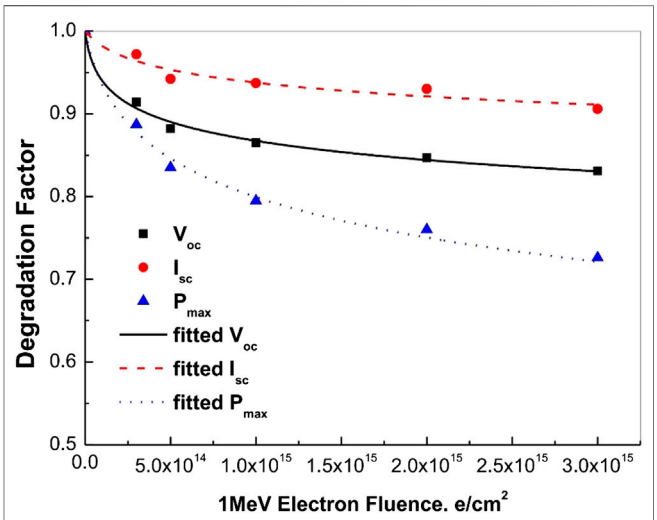

FIGURE 7 | The degradation of electrical parameters of GaInP/GaAs/InGaAs solar cell under 1 MeV electron irradiation with different particle fluence [95].

RADIATION DAMAGE EVALUATION OF SPACE SOLAR CELLS

To obtain better radiation hardened performance, it is essential to explore the radiation damage mechanism of the solar cells. The interaction of high energy charged particles in irradiation environment with the solar cell materials includes ionization and non-ionization (displacement damage) processes [95]. The displacement damage effect is the main reason for the degradation of solar cell performance. It is an effective method to explain the formation, distribution, and evolution of displacement defects after irradiation by different high-energy particles. To examine the

electrical characteristics of solar cells, I-V test, spectral response test, dark characteristic test and photofluorescence intensity test are used. Whereas, to study the displacement defects of multi-junction solar cells, deep level transient spectrum, photofluorescence spectrum, electrofluorescence spectrum and spectral response are employed.

At present, for space solar cells, two assessment methods for evaluating radiation damages of solar cells are available, which are through ground irradiation simulation experiments: equivalent fluence method and equivalent displacement damage method [88]. Both methods are used to study the radiation damage effect and to reveal the degradation mechanism of solar cells. They also provide theoretical guidance and an experimental basis for scientifically predicting the on-orbit behavior of solar cells.

The Equivalent Fluence Method

The equivalent fluence method was proposed by Tada et al. from Jet Propulsion Laboratory, California Institute of Technology [96, 97]. The key point of this approach is the corresponding relative damage coefficient, which is related to the radiation damage effects caused by different types of charged particles with a different energy to relative damage coefficients.

In the first step, the critical fluence (ϕ) of electron or proton irradiation, which is corresponding to the electrical properties of the solar cell degraded to a specified level of its original value (such as 75% of I_{sc0}, V_{oc0}, $P_{\max 0}$), has to be determined according to the experimental results [98]. Then, the relative damage coefficient (RDC) of different energy electron and proton regarding 1 MeV electron and 10 MeV proton is calculated. The ratio of the critical fluence for 1 MeV electrons to the critical fluence for other electron energies is taken as a measure of the RDC of electrons, and similarly, the relative damage coefficients of different proton energies are normalized regarding the 10 MeV proton critical fluence for RDC of protons, as shown in the following equations [88]:

$$\mathrm{RDC}_{x\to 1} = \frac{\phi_e(xMeV)}{\phi_e(1MeV)} \tag{1}$$

$$\mathrm{RDC}_{x\to 10} = \frac{\phi_p(xMeV)}{\phi_p(10MeV)} \tag{2}$$

where ϕ_e and ϕ_p are the critical fluence for electrons and protons.

The next step is using the orbital environment parameters to calculate the corresponding relative damage coefficients for omnidirectional particles on bare cells from the measured values for normally incident particles. By substituting the electron and proton environment parameters under consideration into following integration equations, one can obtain the equivalent 1 MeV electron fluence for the mission in question.

$$\phi_{1\mathrm{MeV,electron,electrons}} = \int \frac{d\phi_e(E)}{dE} D_e(E)dE \tag{3}$$

$$\phi_{1\mathrm{MeV,electron,protons}} = D_{pe}\int \frac{d\phi_p(E)}{dE} D_p(E)dE \tag{4}$$

where $\phi_e(E)$ and $\phi_p(E)$ is the particle fluence of electron and proton, respectively at energy E. $D_e(E)$ and $D_p(E)$ are the relative damage coefficient of electron and proton, respectively. D_{pe} is the proton to electron damage equivalency ratio, which converts 10 MeV proton fluence to an equivalent 1 MeV electron fluence. The calculation result of **Eqs. 3, 4** are the 1 MeV electron fluence normally incident on solar cells that will cause same damage as the selected omnidirectional spectrum. The result of calculated relative damage coefficient for omnidirectional proton irradiation and electron irradiation of GaAs/Ge solar cells are shown in **Figures 8A,B**.

In the equivalent fluence method, it requires a sufficient measurement of data to calculate the RDC and generate a detailed degradation curve, as shown **Figure 4**, which shows eight proton energies (0.05, 0.1, 0.2, 0.3, 0.5, 1.3, and 9.5 MeV) and four electron energies (0.6, 2.4, and 12 MeV). Another relatively simple way of predicting the degradation of a solar cell performance regarding a given electron or proton fluence is using a semi-empirical equation [99]:

$$\frac{P_\phi}{P_0} = 1 - C\cdot\ln\left(1+\frac{\phi}{\phi_x}\right) \tag{5}$$

where P_0 and P_ϕ are the output power (also can be replaced with I_{sc} and V_{oc}) of the solar cell before and after irradiation with different irradiation fluences ϕ, respectively. C and ϕ_x are the fitting parameters for the same structure solar cell using a large amount of experimental data upon specific irradiation particles.

The Displacement Damage Dose Method

The displacement damage dose method was initiated by Naval Research Laboratory (NRL) [100]. The key point of this method is finding the non-ionizing energy loss (NIEL) values for different materials. By using the NIEL method, the radiation fluence of particles is converted into displacement damage dose (*DDD*), and the degradation curve of the electrical parameters of solar cells with the change of *DDD* can be obtained.

The NIEL values of different materials upon different particles with different energies can be calculated by using MULASSIS software [101] or the following equation [102]:

$$\mathrm{NIEL(E)} = \mathrm{n}\cdot\int_{T_d}^{Q_{\max}}\left(\frac{d\sigma(\theta,E)}{d\mathrm{Q}}\right)_E(Q)\cdot G(Q)\cdot Q\cdot d\mathrm{Q} \tag{6}$$

where n is the atomic density of the target material, T_d is the threshold energy to displace atom, $Q_{\max}$ is the maximum energy that can be given to a recoil nuclei by an incident particle of a given energy E, G(Q) is the energy partition function and $(d\sigma/dQ)_E$ the differential interaction cross section. **Figure 9A** shows the calculated results of electron and proton NIEL for GaAs with the energy range from zero up to 200 MeV. The *DDD* induced by irradiation particles can be calculated by the following equation using particle fluence:

$$D_d(E) = \phi(E)\cdot\mathrm{NIEL}(E)\cdot\left[\frac{\mathrm{NIEL}(E_e)}{\mathrm{NIEL}(E_{1MeV})}\right]^{n-1} \tag{7}$$
$$(proton\ n=1, electron\ 1<n<2)$$

where $D_d(E)$ is the *DDD*, $\phi(E)$ is the particle fluence, and NIEL is the non-ionizing energy loss value of the target material. When

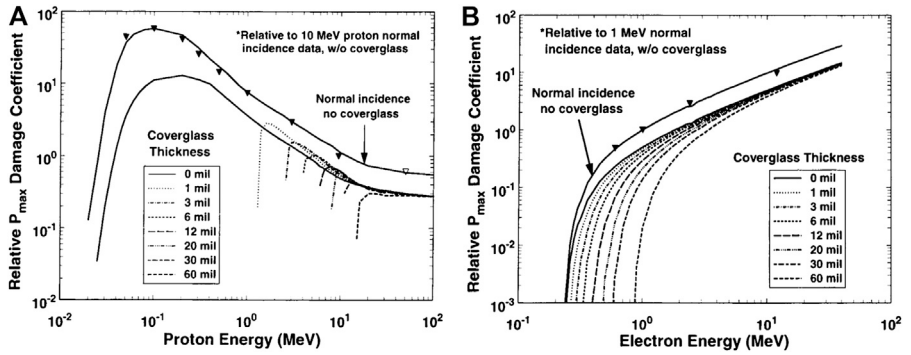

FIGURE 8 | Relative damage coefficient for omnidirectional **(A)** proton and **(B)** electron irradiation of shielded GaAs/Ge solar cells [89].

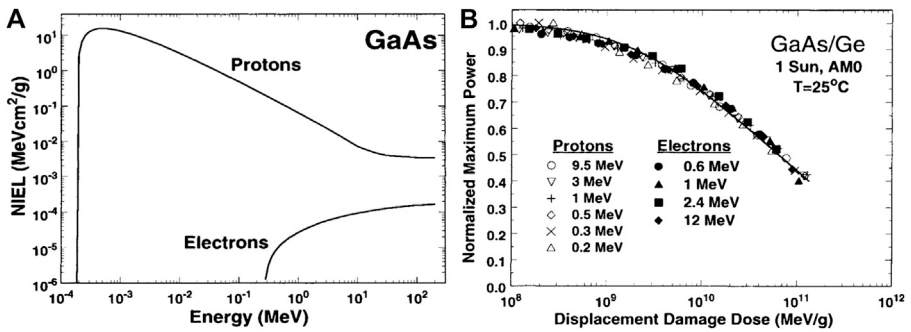

FIGURE 9 | (A) NIEL of electron and proton irradiation in GaAs; **(B)** using the electron to proton damage equivalency factor Rep to fit all of the data from **Figure 4** come a single curve [88].

calculating D_d of proton irradiation, n value is 1, and the n value of electron irradiation is in the range of 1 to 2. Using NIEL of the same particle with different energies, the relative damage coefficient for different energies of a charged particle, i.e. proton, the irradiation can be obtained from using the following equation [99]:

$$D_{x\to 10} = \frac{\mathrm{NIEL}_{(xMeV)}}{\mathrm{NIEL}_{(10MeV)}} \tag{8}$$

where $D_{x\to 10}$ is the X MeV proton to 10 MeV proton relative damage coefficient, and NIEL is the corresponding non-ionization damage energy for different energies. Electron to proton irradiation damage equivalency factor Rep can be calculated by following equation [99]:

$$\mathrm{R}_{ep} = \frac{1}{n}\sum_{n}\frac{Dj}{Di}(n = 1, 2, 3\cdots n) \tag{9}$$

where *Rep* is electron to proton irradiation equivalent damage coefficient, D_j is the actual *DDD* values by using electron irradiation and D_i is the corresponding fitting values of *DDD*. By considering *Rep* degradation curves of electrical parameters of solar cells against the irradiation fluence can be described into a single curve against the D_d. For example, **Figure 9B** shows the re-plot of **Figure 4** using NIEL method. The *DDD* of solar cells in complex electron and proton environment can be calculated by **Eq. 10**, and applied to evaluate the degradation curve of the electrical performance of space solar cells with the *DDD*.

$$D_d = \int \frac{d\phi(E_e)}{dE_p}\cdot \mathrm{NIEL}\left(E_p\right)dE_p + R_{ep}\int \frac{d\phi(E_e)}{dE_e} \cdot \mathrm{NIEL}(E_e)\left[\frac{\mathrm{NIEL}(E_e)}{\mathrm{NIEL}(1MeV)}\right]^{n-1} dE_e \tag{10}$$

Besides, predicting the degradation of a solar cell performance regarding a given electron or proton fluence can also be conducted by using the following semi-empirical equation:

$$\frac{P_{\max}}{P_0} = 1 - C\cdot \ln\left(1 + \frac{D_d}{D_x}\right) \tag{11}$$

where $P_{\max}$ and P_0 are the output power (also can be I_{sc} or V_{oc}) of solar cell before and after irradiation, D_d is the given *DDD* regarding to the given irradiation fluence, respectively. C and D_x are the fitting parameters obtained by on-ground experimental data. **Eq. 4** is more versatile than **Eq. 5** for different kinds of particles by using D_d as variable for given irradiation condition.

Comparing to the equivalent fluence method, the NIEL approach requires fewer experimental measurements to successfully predict the radiation damage of different particles

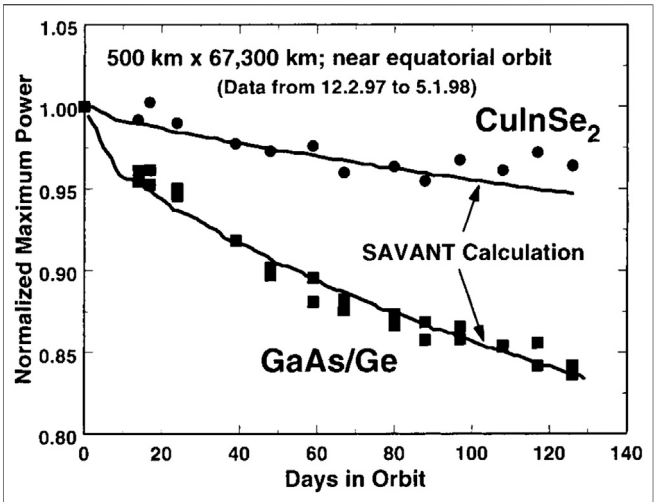

FIGURE 10 | The displacement damage does method measurements for GaAs/Ge and CIS solar cells [88].

at different energies and is easier to implement. Only taking few energies of proton and electron irradiation test data, one can obtain the degradation trends of the electrical properties a solar cell under different particles with different energies and different fluences. Messenger et al. compared the equivalent fluence method and the displacement damage dose method in details and concluded that the key of the displacement damage dose method was NIEL, while the equivalent fluence method needed a lot of experimental data [88]. The displacement damage dose method was successfully applied for predicting on-board solar cell measurements for GaAs/Ge and CIS solar cells at 500 × 67,300 km near equatorial orbit, shown in **Figure 10**.

The Development Trends of Space Solar Cells

There is no doubt that space solar cells should move toward higher efficiency, low cost and better radiation resistance. In this direction, many types of new technologies are trying to solve these problems. Currently, LM triple-junction solar cells are the main stream in space applications. In theory, the solar cell has more junction number has higher efficiency, but it is difficult to increase the number of cell junctions in real cell fabrication. The theoretical limit of N-junction (N for the infinite) solar cells conversion efficiency can reach 68.2% [3]. But the cell fabrication becomes more difficult when the number of junctions is increased, especially for more than 5–6 junctions. The efficiency of multi-junction solar cells from single-junction to six-junction is presented in **Table 4**. Besides, apart from the high cost of III-V materials, the price of GaAs is ten times than that of Si, the growth of III-V materials requires expensive equipment, and hence, the production cost of multijunction solar cells is very high and mostly used in space applications now. Therefore, in the future, the development trends of III-V multijunction solar cells are low-cost, high efficiency, high radiation resistance and simple fabrication method.

CONCLUSION

III-V multijunction solar cells are the primary power supply for space application due to its super high photoelectric conversion efficiency and better radiation resistance. Despite the high fabrication cost, it is widely used in different space applications. New types of space solar cells with new materials and new structures are continuously coming out and the performance characteristics of various space solar cells have been extensively studied. Owing to the development of the balance between the bandgap matching and lattice matching, the structure of solar cells is continuously optimized, more suitable new materials are discovered, and more mature manufacturing processes are utilized. The highest conversion efficiency of solar cells is constantly being refreshed. Comparing to conventional silicon solar cells, the conversion efficiency of III-V multijunction solar cells is significantly improved. Till now, the highest efficiency of crystalline silicon heterojunction solar cell reached 25.6%, and the world record of 47.1% conversion efficiency is achieved by six-junction inverted metamorphic solar cells under 143 suns. Furthermore, lattice-matched GaInP/GaAs/Ge triple junction solar cell fabrication technology is becoming more and more mature with large scale of mass production while keeping the conversion efficiency over 30%.

The space radiation environment is the main threat for in-orbit solar cell performance and lifetime. The high energy particles, such as electrons and protons, induce displacement damages in different regions of solar cell structure and lead to electrical and spectral performance degradation of solar cells. The main reason for the deterioration of space solar cells is that the radiation induced displacement damages forms non-radiative recombination centers and reduces the minority carrier lifetime, and, consequently, results in a reduction of solar cell electrical and spectral parameters. The equivalent fluence method and the displacement damage dose method

TABLE 4 | Comparison of the efficiency of various types of solar cells under concentrated sunlight.

Classification	Efficiency (%)	Area (cm^2)	Intensity (suns)
Si	27.6 ± 1.2 ref. 103	1.00 (aperture area)	92
GaAs	30.5 ± 1.0 ref. 104	0.10043 (designated illumination area)	258
GaInP/GaAs/Ge	40.6 ± 2.0 ref. 97	287 (aperture area)	365
InGaP/GaAs/InGaAs	44.4 ± 2.6 ref. 105	0.1652 (designated illumination area)	302
GaInP/GaAs/GaInAsP/GaInAs (4 J)	46.0 ± 2.2 ref. 73	0.09709 (designated illumination area)	508
AlGaInP/AlGaAs/GaAs/GaInAs/GaInAs/GaInAs (6 J)	47.1 ± 3.2 ref. 8	0.099 (designated illumination area)	143

are two main approaches for evaluating solar cell radiation effects and degradation of cell parameters. Especially, the displacement damage dose method is a more convenient and effective tool. Although the radiation effects of solar cells are widely studied, the radiation damage mechanism of multijunction solar cells with different materials and different structures are not fully explored yet. More experimental and theoretical studies are still needed for further investigating feasible radiation hardening methods.

DATA AVAILABILITY STATEMENT

The data that supports the findings of this study are properly cited with literature and also available from the corresponding author upon reasonable request.

AUTHOR CONTRIBUTIONS

JL, AA, and YL designed the research, conducted the literature review and wrote this manuscript. All authors contributed to the literature review, discussion of the results and edited the manuscript.

FUNDING

This work was supported by a key project of Natural Science Foundation of China (Grant number: 61534008), Basic Research Foundation of Yunnan Province (Grant number: 202001AU070090, 202001AT070086) and Doctoral Start-up Funding of Yunnan Normal University (Grant number: 2019XJLK05/01700205020503040).

REFERENCES

1. Flood DJ. Space photovoltaics - history, progress and promise. *Mod Phys Lett B* (2001) 15(17n19):561–70. doi:10.1142/S0217984901002038
2. Yukinori K, Shoichi N, Shinya T. Recent progress in Si thin film technology for solar cells. *Vacuum* (1991) 42:1035–36. doi:10.1016/0042-207X(91)91251-I
3. Razykov TM, Ferekides CS, Morel D, Stefanakos E, Ullal HS, Upadhyaya HM. Solar photovoltaic electricity: current status and future prospects. *Sol Energy* (2011) 85(8):1580–608. doi:10.1016/j.solener.2010.12.002
4. Dincer F. The analysis on photovoltaic electricity generation status, potential and policies of the leading countries in solar energy. *Renew Sustain Energy Rev* (2011) 15(1):713–20. doi:10.1016/j.rser.2010.09.026
5. Polman A, Knight M, Garnett EC, Ehrler B, Sinke WC. Photovoltaic materials: present efficiencies and future challenges. *Science* (2016) 352:aad4424. doi:10.1126/science.aad4424
6. Green MA. Third generation photovoltaics: solar cells for 2020 and beyond. *Phys E Low-dimens Syst Nanostruct* (2002) 14(1–2):65–70. doi:10.1016/S1386-9477(02)00361-2
7. Yamaguchi M, Takamoto T, Araki K, Ekins-Daukes N. Multi-junction III-V solar cells: current status and future potential. *Sol Energy* (2005) 79(1):78–85. doi:10.1016/j.solener.2004.09.018
8. Geisz JF, France RM, Schulte KL, Steiner MA, Norman AG, Guthrey HL, et al. Six-junction III–V solar cells with 47.1% conversion efficiency under 143 Suns concentration. *Nature Energy* (2020) 5(4):326–35. doi:10.1038/s41560-020-0598-5
9. Patel P, Aiken D, Chumney D, Cornfeld A, Lin Y, Mackos C, et al. Initial results of the monolithically grown six-junction inverted metamorphic multi-junction solar cell. In: IEEE 38th photovoltaic specialist conference part 2; 2012 June 3–8. Austin, TX, USA: IEEE (2012). p. 1–4.
10. Chiu PT, Law DC, Woo RL, Singer SB, Bhusari D, Hong WD, et al. 35.8% space and 38.8% terrestrial 5J direct bonded cells. In: IEEE 40th photovoltaic specialist conference; 2014 June 8–13. Denver, CO, USA: IEEE (2014). p. 11–3.
11. Cariou R, Benick J, Feldmann F, Hohn O, Hauser H, Beutel P, et al. III-V-on-silicon solar cells reaching 33% photoconversion efficiency in two-terminal configuration. *Nature Energy* (2018) 3(4):326–33. doi:10.1038/s41560-018-0125-0
12. Stan M, Aiken D, Cho B, Cornfeld A, Diaz J, Ley V, et al. Very high efficiency triple junction solar cells grown by MOVPE. *J Cryst Growth* (2008) 310(23):5204–8. doi:10.1016/j.jcrysgro.2008.07.024
13. King RR, Karam NH, Ermer JH, Haddad M, Colter P, Isshiki T, et al. Next-generation, high-efficiency III-V multijunction solar cells. In: Conference record of the twenty-eighth IEEE photovoltaic specialists conference; 2000 Sept 15–22. Anchorage, AK, USA: IEEE (2000). p. 998–1001.
14. Geisz JF, Kurtz S, Wanlass MW, Ward JS, Duda A, Friedman DJ, et al. High-efficiency GaInP/GaAs/InGaAs triple-junction solar cells grown inverted with a metamorphic bottom junction. *Appl Phys Lett* (2007) 91:023502. doi:10.1063/1.2753729
15. Geisz JF, Friedman DJ, Ward JS, Duda A, Olavarria WJ, Moriarty TE, et al. 40.8% efficient inverted triple-junction solar cell with two independently metamorphic junctions. *Appl Phys Lett* (2008) 93(12):123505. doi:10.1063/1.2988497
16. Kao YC, Chou HM, Hsu SC, Lin A, Lin CC, Shih ZH, et al. Performance comparison of III–V//Si and III–V//InGaAs multi-junction solar cells fabricated by the combination of mechanical stacking and wire bonding. *Sci Rep* (2019) 9(1):4308. doi:10.1038/s41598-019-40727-y
17. Dimroth F, Grave M, Beutel P, Fiedeler U, Karcher C, Tibbits TND, et al. Wafer bonded four-junction GaInP/GaAs//GaInAsP/GaInAs concentrator solar cells with 44.7% efficiency. *Prog Photovoltaics Res Appl* (2014) 22(3):277–82. doi:10.1002/pip.2475
18. Dharmarasu N, Khan A, Yamaguchi M. Effects of irration on n+p InGaP solar cells. *J Appl Phys* (2002) 91:3306–11. doi:10.1063/1.1445276
19. Ochoa M, Yaccuzzi E, Espinet-Gonzalez P, Barrera M, Barrigon E, Ibarra ML, et al. 10 MeV proton irradiation effects on GaInP/GaAs/Ge concentrator solar cells and their component subcells. *Sol Energy Mater Sol Cell* (2017) 159:576–82. doi:10.1016/j.solmat.2016.09.042
20. Sato S, Miyamoto H, Imaizumi M, Shimazaki K, Morioka C, Kawano K, et al. Degradation modeling of InGaP/GaAs/Ge triple-junction solar cells irradiated with various-energy protons. *Sol Energy Mater Sol Cell* (2009) 93(6–7):768–73. doi:10.1016/j.solmat.2008.09.044
21. Zhang L, Niu P, Li Y, Song M, Zhang J, Ning P, et al. Investigation on high-efficiency $Ga_{0.51}In_{0.49}P/In_{0.01}Ga_{0.99}As$/Ge triple-junction solar cells for space applications. *AIP Adv* (2017) 7:125217. doi:10.1063/1.5006865
22. Maximenko SI, Messenger SR, Hoheisel R, Scheiman D, Gonzalez M, Lorentzen J, et al. Characterization of high fluence irradiations on advanced triple junction solar cells. In: IEEE 39th photovoltaic specialist conference; 2013 June16–21. Tampa, FL, USA: IEEE (2013). p. 2797–800.
23. Hu J, Wu Y, Xiao J, Yang D, Zhang Z. Degradation behaviors of electrical properties of GaInP/GaAs/Ge solar cells under < 200 keV proton irradiation. *Sol Energy Mater Sol Cell* (2008) 92(12):1652–6. doi:10.1016/j.solmat.2008.07.017
24. Gao H, Yang R, Zhang Y. Improving radiation resistance of GaInP/GaInAs/Ge triple-junction solar cells using GaInP back-surface field in the middle subcell. *Materials* (2020) 13(8):1958. doi:10.3390/ma13081958
25. France RM, Espinet-Gonzalez P, Ekins-Daukes NJ, Guthrey H, Steiner MA, Geisz JF. Multijunction solar cells with graded buffer Bragg reflectors. *IEEE J Photovoltaics* (2018) 8(6):1608–15. doi:10.1109/JPHOTOV.2018.2869550

26. Arzbin HR, Ghadimi A. Improving the performance of a multi-junction solar cell by optimizing BSF, base and emitter layers. *Mater Sci Eng B* (2019) 243: 108–14. doi:10.1016/j.mseb.2019.04.001
27. Das AK. Efficiency improvement of p-i-n structure over p-n structure and effect of p-Layer and i-Layer properties on electrical measurements of gallium nitride and indium nitride alloy based thin film solar cell using AMPS-1D. *IOSR J Appl Phys* (2015) 7(2):08–15. doi:10.9790/4861-07220815
28. Fang M, Fei T, Bai M, Guo Y, Lv J, Quan R, et al. Annealing effects on GaAs/Ge solar cell after 150 keV proton irradiation. *Int J Photoenergy* (2020) 2020:1–8. doi:10.1155/2020/3082835
29. Sharma S, Jain KK, Sharma A. Solar cells: in research and applications—a review. *Mater Sci Appl* (2015) 06(12):1145–55. doi:10.4236/msa.2015.612113
30. Kabir E, Kumar P, Kumar S, Adelodun AA, Kim K-H. Solar energy: potential and future prospects. *Renew Sustain Energy Rev* (2018) 82(1):894–900. doi:10.1016/j.rser.2017.09.094
31. Snaith HJ. Perovskites: the emergence of a new era for low-cost, high-efficiency solar cells. *J Phys Chem Lett* (2013) 4(21):3623–30. doi:10.1021/jz4020162
32. Hagfeldt A, Boschloo G, Sun L, Kloo L, Pettersson H. Dye-sensitized solar cells. *Chem Rev* (2010) 110(11):6595–663. doi:10.1021/cr900356p
33. Hoppe H, Sariciftci NS. Organic solar cells: an overview. *J Mater Res* (2004) 19(7):1924–7945. doi:10.1557/JMR.2004.0252
34. Kayes BM, Zhang L, Ding IK, Higashi GS. Flexible thin-film tandem solar cells with > 30% efficiency. *IEEE J Photovoltaics* (2014) 4(2):729–33. doi:10.1109/JPHOTOV.2014.2299395
35. Yamaguchi M, Takamoto T, Araki K, Ekins-Daukes N. Multi- junction III-V solar cells: current status and future potential. *Sol Energy* (2005) 79(1):78–85. doi:10.1016/j.solener.2004.09.018
36. Bouisset P, Nguyen VD, Akatov YA, Siegrist M, Parmentier N, Archangelsky VV, et al. Quality factor and does equivalent investigations aboard the soviet space station MIR. *Adv Space Res* (1992) 12(2–3):363–7. doi:10.1016/0273-1177(92)90130-P
37. Moon S, Kim K, Kim Y, Heo J, Lee J. Highly efficient single-junction GaAs thin-film solar cell on flexible substrate. *Sci Rep* (2016) 6:30107. doi:10.1038/srep30107
38. Stephen P, Steven J, Mark S, Keith A. Assessment of MOCVD- and MBE-growth GaAs for high-efficiency solar cell applications. *IEEE Trans Electron Dev* (1990) 37(2):469–77. doi:10.1109/16.46385
39. Iles PA, Yeh Y-CM, Ho FH, Chu C-L, Cheng C. High-efficiency (> 20% AMO) GaAs solar cells - grown on inactive-Ge substrates. *IEEE Electron Device Lett* (1990) 11(4):140–2. doi:10.1109/55.61775
40. Yamaguchi M, Lee KH, Araki K, Kojima N, Yamada H, Katsumata Y. Analysis for efficiency potential of high-efficiency and next-generation solar cells. *Prog Photovoltaics Res Appl* (2018) 26(8):543–52. doi:10.1002/pip.2955
41. Gaddy EM. Cost performance of multi-junction, gallium arsenide, and silicon solar cells on spacecraft. In: Conference record of the twenty fifth IEEE photovoltaic specialists conference; 1996 May 13–17. Washington, DC, USA: IEEE (1996). p. 293–6.
42. King RR, Fetzer CM, Colter PC, Edmondson KM, Ermer JH, Cotal HL, et al. High-efficiency space and terrestrial multijunction solar cells through bandgap control in cell structures. In: Conference record of the twenty-ninth IEEE photovoltaic specialists conference; 2002 May 19–24. New Orleans, LA, USA: IEEE (2002). p. 776–81.
43. Messenger SR, Burke EA, Walters RJ, Warner JH, Summers GP. Using SRIM to calculate the relative damage coefficients for solar cells. *Prog Photovoltaics Res Appl* (2005) 13(2):115–23. doi:10.1002/pip.608
44. Nishioka K, Takamoto T, Agui T, Kaneiwa M, Uraoka Y, Fuyuki T. Evaluation of InGaP/InGaAs/Ge triple-junction solar cell and optimization of solar cell's structure focusing on series resistance for high-efficiency concentrator photovoltaic systems. *Sol Energy Mater Sol Cell* (2006) 90(9):1308–21. doi:10.1016/j.solmat.2005.08.003
45. Guter W, Schoene J, Philipps SP, Steiner M, Siefer G, Wekkeli A, et al. Current-matched triple-junction solar cell reaching 41.1% conversion efficiency under concentrated sunlight. *Appl Phys Lett* (2009) 94(22):223504. doi:10.1063/1.3148341
46. Kondow M, Uomi K, Niwa A, Kitatani T, Watahiki S, Yazawa Y. GaInNAs: a novel material for long-wavelength-range laser diodes with excellent high-temperature performance. *Jpn J Appl Phys* (1996) 35(No 2s):1273. doi:10.1143/JJAP.35.1273
47. Lew K, Yoon S, Wang H, Wicaksono S, Gupta J, McAlister S, et al. GaAsNSb-base GaAs heterojunction bipolar transistor with a low turn-on voltage. *J Vac Sci Technol B* (2006) 24(3):1308. doi:10.1116/1.2200376
48. Tansu N, Kirsch NJ, Mawst LJ. Low-threshold-current-density 1300-nm dilute-nitride quantum well lasers. *Appl Phys Lett* (2002) 81(14):2523. doi:10.1063/1.1511290
49. Polojärvi V, Aho A, Tukiainen A, Raappana M, Aho M, Schramm A, et al. Influence of As/group-III flux ratio on defects formation and photovoltaic performance of GaInNAs solar cells. *Sol Energy Mater Sol Cells* (2016) 149: 213–20. doi:10.1016/j.solmat.2016.01.024
50. Friedman DJ, Kurtz SR. Breakeven criteria for the GaInNAs junction in GaInP/GaAs/GaInNAs/Ge four-junction solar cells. *Prog Photovoltaics Res Appl* (2002) 10(5):331–44. doi:10.1002/pip.430
51. Kurtz S, King RR, Edmondson KM, Friedman DJ, Karam NH. 1-MeV-electron irradiation of GaInAsN cells. In: Conference record of the twenty ninth IEEE photovoltaic specialists conference; 2002 May 19–24. New Orleans, LA, USA: IEEE (2002). p. 1006–9.
52. Miyashita N, Shimizu Y, Kobayashi N. Fabrication of GaInNAs-based solar cells for application to multi-junction tandem solar cells. In: Conference record of the 2006 IEEE 4th world conference on photovoltaic energy conversion; 2006 May 7–12. Hawaii, USA: IEEE (2006). p. 869.
53. Sailai M, Qiqi L, Aierken A, Heini M, Fan Zhao X, Ting Hao R, et al. 1 MeV electron irradiation and post-annealing effects of GaInAsN diluted nitride alloy with 1 eV bandgap energy. *Thin Solid Films* (2020) 709:138237. doi:10.1016/j.tsf.2020.138237
54. Jackrel DB, Bank SR, Yuen HB, Wistey MA, Harris JS, Ptak AJ, et al. Dilute nitride GaInNAs and GaInnAsSb solar cells by molecular beam epitaxy. *Jpn J Appl Phys* (2007) 101(11):114916. doi:10.1063/1.2744490
55. Han XX, Suzuki H, Lee JH, Kojima N, Ohshita Y, Yamaguchi M. N incorporation and optical properties of GaAsN epilayers on (311) A/B GaAs substrates. *Jpn J Appl Phys* (2011) 44(1):015402. doi:10.1088/0022-3727/44/1/015402
56. Miyashita N, Ahsan N, Islam M, Okada Y. Study on the device structure of GaInNAs (Sb) based solar cells for use in 4-junction tandem solar cells. In: Conference record of the 38th IEEE photovoltaic specialists conference; 2012 June 3–8. Austin, USA: IEEE (2012). p. 000954.
57. Miyashita N, Ahsan N, Okada Y. Effect of antimony on uniform incorporation of nitrogen atoms in GaInNAs films for solar cell application. *Sol Energy Mater Sol Cells* (2013) 111:127–32. doi:10.1016/j.solmat.2012.12.036
58. Han XX, Tanaka T, Kojima N, Ohshita Y, Yamaguchi M, Sato S. Growth orientation dependent photoluminescence of GaAsN alloys. *Appl Phys Lett* (2012) 100(3):032108. doi:10.1063/1.3679079
59. Andreev VM. IId-1-GaAs and high-efficiency space cells. *Pract Handb Photovoltaics Fundamentals Appl* (2003) 417–33. doi:10.1016/B978-185617390-2/50017-9
60. Gee JM, Virshup GF. A 31%-efficient GaAs/silicon mechanically stacked, multijunction concentrator solar cell. In: Conference record of the 20th IEEE photovoltaic specialists conference; 1988 Sept 26–30. Las Vegas, NV: IEEE (1988). p. 754–8.
61. Yazawa Y, Tamura K, Watahiki S, Kitatani T, Ohtsuka H, Warabisako T. Three-junction solar cells comprised of a thin-film GaInP/GaAs tandem cell mechanically stacked on a Si cell. In: Conference record of the 26th IEEE photovoltaic specialists conference; 1997 Sept 29–Oct 3. Anaheim, CA, USA: IEEE (1997). p. 899–902.
62. Essig S, Ward S, Steiner MA, Friedman DJ, Geisz JF, Stradins P, et al. Progress towards a 30% efficient GaInP/Si tandem solar cell. *Energy Procedia* (2015) 77: 464–9. doi:10.1016/j.egypro.2015.07.066
63. Zhao L, Flamand G, Poortmans J. Recent progress and spectral robustness study for mechanically stacked multi-junction solar cells. *AIP Conf Proc* (2010) 1277(1):284. doi:10.1063/1.3509212
64. Baba M, Makita K, Mizuno H, Takato H, Sugaya T, Yamada N. Feasibility study of two terminal tandem solar cellsintegrated with smart stack, areal current matching,and low concentration. *Prog Photovoltaics Res Appl* (2016) 25(3):255–63. doi:10.1002/pip.2856

65. Mizuno H, Makita K, Matsubara K. Electrical and optical interconnection for mechanically stacked multi-junction solar cells mediated by metal nanoparticle arrays. *Appl Phys Lett* (2012) 101(19):191111. doi:10.1063/1.4766339
66. Yoshidomi S, Furukawa J, Hasumi M, Sameshima T. Mechanical stacking multi junction solar cells using transparent conductive adhesive. *Energy Procedia* (2014) 60:116–22. doi:10.1016/j.egypro.2014.12.352
67. Makita K, Mizuno H, Tayagaki T, Aihara T, Oshima R, Shoji Y, et al. III-V//Si multijunction solar cells with 30% efficiency using smart stack technology with Pd nanoparticle array. *Prog Photovoltaics Res Appl* (2019) 28(1):16–24. doi:10.1002/pip.3200
68. Tanabe K, Fontcuberta i Morral A, Atwater HA, Aiken DJ, Wanlass MW. Direct-bonded GaAs/InGaAs tandem solar cell. *Appl Phys Lett* (2006) 89(10):102–6. doi:10.1063/1.2347280
69. Dharmarasu N, Yamaguchi M, Khan A, Yamada T, Tanabe T, Takagishi S, et al. High-radiation-resistant InGaP, InGaAsP, and InGaAs solar cells for multijuction solar cells. *Appl Phys Lett* (2001) 79(15):2399. doi:10.1063/1.1409270
70. Dai P, Ji L, Tan M, Uchida S, Wu Y, Abuduwayiti A, et al. Electron irradiation study of room-temperature wafer-bonded four-junction solar cell grown by MBE. *Sol Energy Mater Sol Cell* (2017) 171:1181–22. doi:10.1016/j.solmat.2017.06.046
71. Essig S, Benick J, Schachtner M, Wekkeli A, Hermle M, Dimroth F, et al. Wafer-bonded GaInP/GaAs//Si solar cells with 30% efficiency under concentrated sunlight. *IEEE J Photovoltaics* (2015) 5(3):977–81. doi:10.1109/JPHOTOV.2015.2400212
72. Dimroth F, Roesener T, Essig S, Weuffen C, Wekkeli A, Oliva E, et al. Comparison of direct growth and wafer bonding for the fabrication of GaInP/GaAs dual-junction solar cells on silicon. *IEEE J Photovoltaics* (2014) 4(2):620–5. doi:10.1109/JPHOTOV.2014.2299406
73. Dimroth F, Tibbits TND, Niemeyer M, Predan F, Beutel P, Karcher C, et al. Four-junction wafer-bonded concentrator solar cells. *IEEE J Photovoltaics* (2016) 6(1):343–9. doi:10.1109/JPHOTOV.2015.2501729
74. Sinharoy S, Patton MO, Valko TM, Weizer VG. Progress in the development of metamorphic multi-junction III-V space solar cells. *Prog Photovoltaics Res Appl* (2002) 10(6):427–32. doi:10.1002/pip.449
75. France RM, Geisz JF, Garcia I, Steiner MA, McMahon WE, Friedman DJ, et al. Design flexibility of ultrahigh efficiency four-junction inverted metamorphic solar cells. *IEEE J Photovoltaics* (2016) 6(2):578–83. doi:10.1109/JPHOTOV.2015.2505182
76. Long J, Xiao M, Huang X, Xing Z, Li X, Dai P, et al. High efficiency thin film GaInP/GaAs/InGaAs inverted metamorphic (IMM) solar cells based on electroplating process. *J Cryst Growth* (2019) 513:38–42. doi:10.1016/j.jcrysgro.2019.02.057
77. Aierken A, Fang L, Heini M, Zhang QM, Li ZH, Zhao XF, et al. Effects of proton irradiation on upright metamorphic GaInP/GaInAs/Ge triple junction solar cells. *Sol Energy Mater Sol Cell* (2018) 185:36–44. doi:10.1016/j.solmat.2018.04.035
78. France RM, Geisz JF, Steiner MA, Friedman DJ, Ward JS, Olson JM, et al. Pushing inverted metamorphic multijunction solar cells toward higher efficiency at realistic operating conditions. *IEEE J Photovoltaics* (2013) 3(2):893–8. doi:10.1109/JPHOTOV.2013.2239358
79. Garcia I, France RM, Geisz JF, McMahon WE, Steiner MA, Johnston S, et al. Metamorphic III–V solar cells: recent progress and potential. *IEEE J Photovoltaics* (2016) 6(1):366–73. doi:10.1109/JPHOTOV.2015.2501722
80. Guter W, Dunzer F, Ebel L, Hillerich K, Koestler W, Kubera T, et al. Space solar cells-3G30 and next generation radiation hard products. *11th Eur Space Power Conf* (2017) 16:03005. doi:10.1051/e3sconf/20171603005
81. Yoshikawa K, Kawasaki H, Yoshida W, Irie T, Konishi K, Nakano K, et al. Silicon heterojunction solar cell with interdigitated back contacts for a photoconversion efficiency over 26%. *Nature Energy* (2017) 2(5):17032. doi:10.1038/nenergy.2017.32
82. Kayes MK, Nie H, Twist R, Spruytte SG, Reinhardt F, Kizilyalli IC, et al. 27.6% conversion efficiency, a new record for single-junction solar cells under 1 sun illumination. In: 37th IEEE photovoltaic specialists conference; 2011 June 19–24. Seattle, WA, USA: IEEE (2011). p. 4–8.
83. Chen Z, Zheng X, Li Z, Wang P, Rong X, Wang T, et al. Positive temperature coefficient of photovoltaic efficiency in solar cells based on InGaN/GaN MQWs. *Appl Phys Lett* (2016) 109(6):062104. doi:10.1063/1.4960765
84. Yamaguchi M. Multi-junction solar cells and novel structures for solar cell applications. *Phys E Low Dimens Syst Nanostruct* (2002) 14(1–2):84–90. doi:10.1016/S1386-9477(02)00362-4
85. Bhuiyan AG, Sugita K, Hashimoto A, Yamamoto A. InGaN Solar Cells: present state of the art and important challenges. *IEEE J Photovoltaics* (2012) 2(3):276–93. doi:10.1109/JPHOTOV.2012.2193384
86. Hamache A, Sengouga N, Meftah A, Henini M. Modeling the effect of 1MeV electron irradiation on the performance of n+–p–p+ silicon space solar cells. *Radiat Phys Chem* (2016) 123:103–8. doi:10.1016/j.radphyschem.2016.02.025
87. Rehman AU, Lee SH, Lee SH. Silicon space solar cells: progression and radiation-resistance analysis. *J Kor Phys Soc* (2016) 68(4):593–8. doi:10.3938/jkps.68.593
88. Messenger SR, Summers GP, Burke EA, Walters RJ, Xapsos MA. Modeling solar cell degradation in space: a comparison of the NRL displacement damage dose and the JPL equivalent fluence approaches. *Prog Photovoltaics Res Appl* (2001) 9(2):103–21. doi:10.1002/pip.357
89. Hu JM, Wu Y-Y, Zhang Z, Yang DZ, He SY. A study on the degradation of GaAs/Ge solar cells irradiated by <200keV protons. *Nucl Instrum Methods Phys Res Sect B Beam Interact Mater Atoms* (2008) 266(2):267–70. doi:10.1016/j.nimb.2007.11.010
90. Sharps PR, Aiken DJ, Stan MA, Thang CH, Fatemi N. Proton and electron radiation data and analysis of GaInP2/GaAs/Ge solar cells. *Prog Photovoltaics Res Appl* (2002) 10(6):383–90. doi:10.1002/pip.444
91. Wang R, Lu M, Yi T-C, Yang K, Ji X-X. Effects of 1.0–11.5 MeV electron irradiation on GaInP/GaAs/Ge triple-junction solar cells for space applications. *Chin Phys Lett* (2014) 31(8):086103. doi:10.1088/0256-307X/31/8/086103
92. Takamoto T, Juso H, Ueda K, Washio H, Yamaguchi H. IMM triple-junction solar cells and modules optimized for space and terrestrial conditions. In: IEEE 44th photovoltaic specialist conference; 2017 June 25–30. Washington, DC, USA: IEEE (2017). p. 3506–10.
93. Imaizumi M, Nakamura T, Takamoto T, Ohshima T, Tajima M. Radiation degradation characteristics of component subcells in inverted metamorphic triple-junction solar cells irradiated with electrons and protons. *Prog Photovoltaics Res Appl* (2017) 25(2):161–74. doi:10.1002/pip.2840
94. Zhang Y, Wu Y, Zhao H, Sun C, Xiao J, Geng H, et al. Degradation behavior of electrical properties of inverted metamorphic tri-junction solar cells under 1 MeV electron irradiation. *Sol Energy Mater Sol Cell* (2016) 157:861–6. doi:10.1016/j.solmat.2016.08.006
95. Allam EE, Inguimbert C, Addarkaoui S, Meulenberg A, Jorio A, Zorkani I. NIEL calculations for estimating the displacement damage introduced in GaAs irradiated with charged particles. *IOP Conf Ser Mater Sci Eng* (2017) 186:012005. doi:10.1088/1757-899X/186/1/012005
96. Tada HY, Carter JR, Anspaugh BE. *Solar cell radiation handbook*. Pasadena, USA: Jet Propulsion Laboratory (1982).
97. Green MA, Keevers MJ, Thomas I, Lasich JB, Emery K, King RR. 40% efficient sunlight to electricity conversion. *Prog Photovoltaics Res Appl* (2015) 23(6):685–591. doi:10.1002/pip.2612
98. Anspaugh BE. *GaAs solar cell radiation handbook*. Pasadena, USA: Jet Propulsion Laboratory (1996).
99. Zhao XF, Aierken A, Heini M, Tan M, Wu YY, Lu SL, et al. Degradation characteristics of electron and proton irradiated InGaAsP/InGaAs dual junction solar cell. *Sol Energy Mater Sol Cell* (2020) 206:110339. doi:10.1016/j.solmat.2019.110339
100. Walters RJ, Summers GP. Analysis and modeling of the radiation response of multijunction space solar cells. In: Conference record of the twenty-eighth IEEE photovoltaic specialists conference; 2020 Sept 15–22. Anchorage, AK, USA: IEEE (2000). p. 1092–7.
101. Lei F, Truscott PR, Dyer CS, Quaghebeur B, Heynderickx D, Nieminen P, et al. MULASSIS: a geant4-based multilayered shielding simulation tool. *IEEE Trans Nucl Sci* (2002) 49(6):2788–93. doi:10.1109/TNS.2002.805351

102. Inguimbert C, Gigante R. NEMO: a code to compute NIEL of protons, neutrons, electrons, and heavy ions. *IEEE Trans Nucl Sci* (2006) 53(4): 1967–72. doi:10.1109/TNS.2006.880926
103. Slade A, Garboushian V. 27.6% Efficient silicon concentrator solar cells for mass production. In: Technical digest, *15th international photovoltaic science and engineering conference*; 2005 Oct 10–15. Shanghai, China: CRES (2005). p. 701.
104. Green MA, Hishikawa Y, Dunlop ED, Levi DH, Hohl-Ebinger J, Yoshita M, et al. Solar cell efficiency tables (Version 53). *Prog Photovoltaics Res Appl* (2019) 27(1):3–12. doi:10.1002/pip.3102
105. Green MA, Dunlop ED. Solar cell efficiency tables (Version 55). *Prog Photovoltaics Res Appl* (2019) 28(1):3–15. doi:10.1002/pip.3228

Conflict of Interest: The authors declare that the research was conducted in the absence of any commercial or financial relationships that could be construed as a potential conflict of interest.